Deposition of Manganese Oxide Films on Stainless Steel by a Reactive Evaporation

Masaaki Isai[a] and Hiroshi Fujiyasu
Department of Electrical and Electronic Engineering,Shizuoka
University, 3-5-1 Johoku, Hamamatsu, Shizuoka, Japan 432-8561
[a]Fax:053-478-1105, e-mail: isai@eng.shizuoka.ac.jp
Takayuki Kashiwakura
Department of Electrical and Electronic Engineering,Utsunomiya
University, 7-1-2 Yohtoh, Utsunomiya, Tochigi, Japan 321-8585

Manganese (Mn) oxide films for lithium secondary batteries were prepared using the reactive evaporation method. A molybdenum (Mo) separator was introduced in the bottom of the Mn crucible. It can successfully isolate Mn evaporant from incoming oxygen (O_2) atoms. Actually the deposition rate decreases gradually as the deposition run increases, especially under the large O_2 atmosphere. It was found that hausmannite (Mn_3O_4) films could be prepared with the deposition rate between 3 - 10 Å/s. The XRD data showed that the (103) orientation has a maximum peak in this deposition rate area. It means that an optimum evaporation condition could be within this deposition rate area. It is found that the film composition depends on the O_2 flow rate, deposition rate, and substrate temperature (T_{sub}). The variation of hausmannite structure related to the deposition rate was investigated under the condition of O_2 flow rate of 5 sccm and the aperture size of the separator of 6 mm.
Key words: Li secondary batteries, Mn oxide films, reactive evaporation

I. INTRODUCTION

The electric vehicles and hybrid cars have been seen frequently in the suburbs as well as in towns. Many people have been focusing their attention to them because of environmental concerns as well as depletion of petroleum resources. The lithium secondary batteries, fuel cells and others[1,2] have been considered as power sources for them. A tight race (a hot competition) of the development of power sources has continued for a long time. A combination of manganese (Mn) oxide and lithium (Li) was chosen in this study as the positive and negative electrodes, respectively. Mn oxide is one of the best materials for the positive electrode in the Li secondary batteries.[3] Mn is more abundant and less expensive than cobalt (Co), so that the overall cost would be minimized if $LiMn_2O_4$ is used as the positive electrode. Toxicity, if any, or recycling is already well known. The operating voltage of 3～5V could be obtained with this material.

Almost all the oxide powders for positive electrodes are prepared by the sintering method.[4-7] The materials have usually inferior electric conductivities. In this study we focused on the thin film technology, so called hotwall epitaxy, to improve the electric conductivity. Mn oxide films were prepared by using reactive evaporation method.[8-22]

A striking problem is the oxidation of Mn evaporant during the reactive evaporation. It deteriorates the Mn deposition rate run by run. To overcome this deficiency, a molybdenum (Mo) sheet with a small hole was set just over the Mn evaporant. It is called hereafter as the Mo separator. The oxidation of the Mn evaporant was successfully prevented by this method.[18-20] It was found that hausmannite (Mn_3O_4) films could be prepared only with the restricted conditions. The key parameters which govern the film properties were investigated.

The purpose of the present work is to investigate the variation of crystal structure on the deposition run. The composition of hausmannite films was also examined with X-ray Diffraction (XRD) and X-ray photoelectron spectroscopy (XPS) analyses.

II. EXPERIMENT

Deposition apparatus is shown in Fig. 1 (a). Mn was evaporated in the oxygen atmosphere. The O_2 flow rate was controlled by a mass flow controller. The flow rate was fixed to 5 sccm. Mn oxide film was deposited on a stainless steel sheet substrate by hotwall epitaxy. The stainless steel crucible was resistively heated. The temperatures of the upper and lower parts of the crucible referred to as T_{wall} and T_{source}, respectively. They were measured by the thermocouples attached on the surface of crucible. The substrate temperature (T_{sub}) was not controlled in this study. Actually the T_{sub} is gradually increased at the beginning of the first deposition run. After about 10 minutes, the T_{sub} is saturated at 410 to 470 °C under the condition of T_{sub} of 900 °C and T_{source} between 930 to 970 °C.

(a)

OXYGEN   VACUUM

(b)

crucible
(stainless steel)
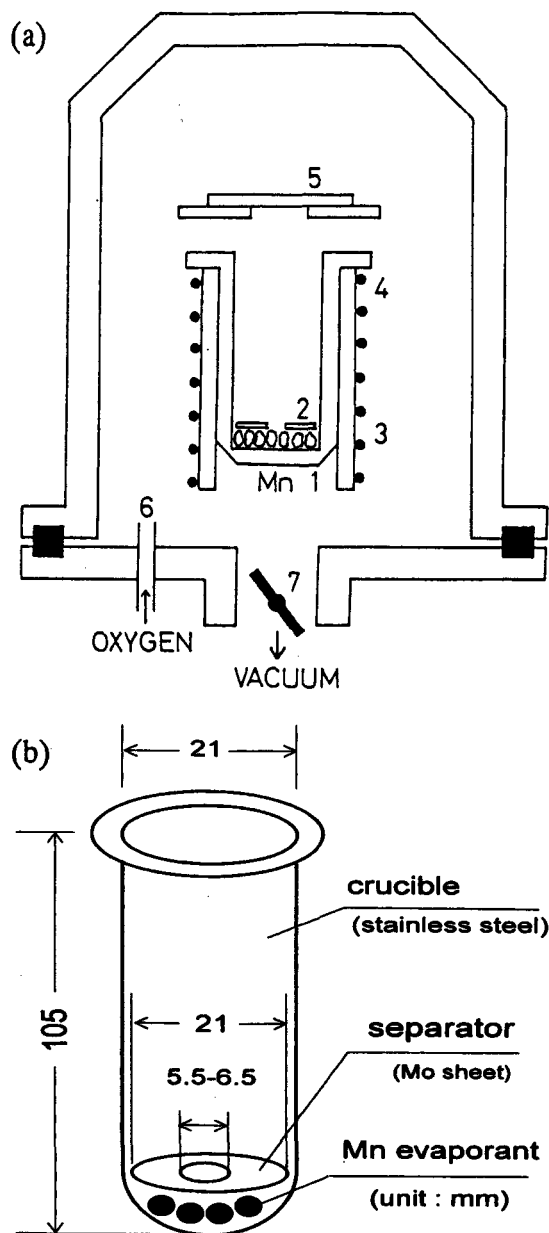
separator
(Mo sheet)

Mn evaporant
(unit : mm)

Fig. 1(a). Schematic of the apparatus. 1: Stainless steel crucible for Mn evaporation. 2: A molybdenum (Mo) sheet with a hole is set in the bottom of the crucible. 3: Hotwall heater for Mn evaporant. 4: Quartz tube with W heater wire. 5: Stainless steeel substrate. 6: O_2 inlet. 7: Main valve to control the O_2 atmosphere. (b) Schematic of the Mn crucible. A Mo sheet with a hole is set in the bottom of the crucible. It is called as the separator in the text.

The Mo separator keeps Mn evaporant off the oxygen atoms. The hole size governs the oxidation of Mn evaporant as well as the Mn deposition rate. An aperture size of 6 mm ϕ was the best compromise between the Mn oxidation and Mn deposition rate under the O_2 flow rate of 5 sccm. A 1g of metallic Mn was charged in the crucible and was renewed after five

succeeding deposition runs.

The Mn oxide films prepared were subjected to XRD and XPS evaluations. In order to obtain crystallographic information, a x-ray photoelectron spectroscopy for some films was carried out in an ULVAC-PHI ESCA1600C with a 15-keV Mg K_α ray source. The spot size on the sample for collecting photoelectrons was 0.8mm ϕ. The sputter gun was set to 3 kV Ar⁺ ions. XRD measurements for some samples were also performed on a RIGAKU Rotaflex 12kW system with a CN2173D6 goniometer. The film thickness was measured by an optical method (interference fringes) and a gravimetric method. A SLOAN DEKTAK II surface profiler was used for an optical method. The Mn density of 7.44 g/cm³ was used to calculate the film thickness in the case of gravimetric method.

III. RESULTS AND DISCUSSION

Figure 2 shows a curve of deposition rate vs. deposition run for Mn oxide films deposited with the O_2 flow rate of 5 sccm. The deposition rate decreased gradually as the deposition run increased. The Mn evaporant was scarecely oxidized in oxygen atmosphere. This shows the effectiveness of the Mn separator: it can effectively keep oxygen off the Mn evaporant. The deposition rate is significantly deteriorated after one deposition run if the Mo separator is not used. The five films were used for the XRD and XPS analyses after thickness measurement.
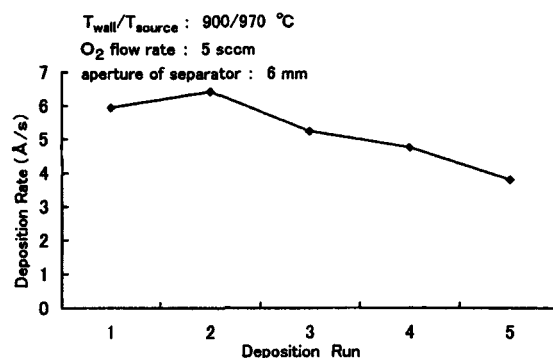
Fig. 2. Variation of Mn deposition rate on the deposition run under the O_2 flow rate of 5 sccm.

Figure 3 shows the XRD patterns for the films. The film composition could be identified by comparing a series of crystal planes with that of ASTM cards. A Mn_3O_4 structure has a series of (101), (112), (103), (211) and (224) planes.[23] These films are so called hausmannite. They could be prepared under the deposition rate between 3 and 10 Å/s.[15-22] A first run film had MnO phases as an extra phase. Films containing more MnO were deposited with other rates than 3-10 Å/s.

Fig. 3. Variation of crystal structures of these films examined by the XRD.

Figures 4(a), (b) and (c) show XPS profiles for Mn oxide films. The stoichiometry of films was examined by the XPS analysis. The film composition was measured before and after Ar ion sputtering the surface of the film for 1 hour. The sensitivity factors of Mn2p, O1s, C1s were 2.600, 0.660 and 0.250, respectively.[24] The film of fourth deposition run referred to as sample 4.

Figure 4(a) is an XPS spectrum obtained after sputtering the surface of with Ar-beams for 1h. Figure 4(b) shows the Mn2p peak for the Ar-sputtered sample 4. Several peaks can be identified as follows.[24,25] The peak at 632 eV comes from the satellite of Mg K_a. The peak at 641 eV comes from Mn $2p3/2$ of MnO_x. The peak at 648 eV comes from the satellite of Mn $2p3/2$ of MnO. The peak at 654 eV comes from Mn $2p1/2$ of MnO_x. The peak at 660 eV comes from the satellite of Mn $2p1/2$ of MnO. These MnO peaks only evolved after Ar-sputtering. It is seemed that the main peaks of MnO_x and MnO have quite similar binding energies. The peak at 672 eV comes from energy loss structure but, it could not be identified yet.

Fig. 4. (a) An XPS survey spectrum of sample 4 after Ar ion sputtering the surface of the film for 1 hour. (b) Mn 2p peaks. (c) O1s peaks examined with XPS analysis.

Figure 4(c) shows O1s peaks for the Ar –sputtered sample 4. The peak at 532 eV comes from the satellite of Mg k_a. The peak at 530 eV comes from O 1s of MnO_x. It is seemed that the peak at 532 eV comes from the oxygen or hydrooxides[25] adsorbed on the film surface after deposition. The peak height of the shoulder at around 532 eV decreased after the etching.

The composition of Mn oxide films depends on the Mn deposition rate, O_2 flow rate and T_{sub}.[15-22] The O_2 flow rate and T_{wall} were fixed at 5 sccm and 900 °C, respectively throughout this study. The key factor, which governs the film composition, is exactly the Mn deposition rate and the T_{sub}. In these circumstances, the Mn deposition rate depends on T_{source} and the aperture size of the Mo separator. T_{source} was maintained at 970 °C through this experiment. The Mn deposition rate dependence on the film properties was shown in early papers.[19,20]

The film composition of the first run was differed from others as shown in Fig. 3. The reason could be examined by the variation of T_{sub} during the first deposition run. The substrate temperature was not

controlled in this study. The substrate holder is located at 30 mm above the crucible just before the deposition starts. The substrate reached temperatures of 410 ~ 470 °C after about ten min from the beginning of deposition, and was kept to the temperatures until fifth depositon run because substrate was heated with radiations from T_{wall}, T_{source} and incoming Mn atoms.

The mean free path of photoelectrons is less than 1 nm. So, the XPS analysis could give information on the averaged data of several mono-layers from film surface. No matrix correction was used in the composition analysis. In the case of XRD analysis, the analyzing depth (area) spreads all the film thickness. The discrepancy between XRD and XPS analysis seemed to be due to the difference of analyzing depth (area). Further analysis and better understanding are on the way.

Preparation of $LiMn_2O_4$ films is now undergone with co-depositing lithium during the Mn_3O_4 deposition. One of the problems to be solved is to keep the crystallinity of hausmannite structure. We hope to report on these aspects later. We are convinced that the idea shown in the present work could be equally applicable for the preparation of other oxide films.

IV. CONCLUSION

The Mn oxide films were prepared by the reactive evaporation method. A molybdenum sheet with a small hole was introduced in the crucible to prevent the oxidation of Mn evaporant. An aperture size of 6 mm ϕ was the best compromise between the Mn oxidation and Mn deposition rate under the O_2 flow rate of 5 sccm. The oxidation of the Mn evaporant was successfully prevented by this method.

The (103) oriented crystalline Mn oxide films with hausmannite (Mn_3O_4) structure could be prepared with the deposition rate between 3 and 10 Å/s.

This study helps us to understand the reactive evaporation process of Mn oxide films. This technique could be equally applicable for the preparation of other oxide films.

REFERENCES

1. J. Desilvestro and O. Haas, J. Electrochem. Soc. 137, 5C (1990).
2. R. Koksbang, J. Barker, H. Shi, and M. Y. Saidi, Solid State Ionics 84,1 (1996).
3. S.Basu, U. S. Patent 4, 423, 125 (1983).
4. J. C. Hunter, J. Solid State. Chem. 39, 142 (1981).
5. M. M. Thackeray, W. I. F. David, P. G. Bruce, and J. B. Goodenough, Mater. Res. Bull. 18, 461 (1983).
6. W. I. F. David, M. M. Thackeray, L. A. De Picciotto, and J. B. Goodenough, J. Solid State Chem. 67, 316 (1987).
7. M. M. Thackeray, A de Kock, M. H. Rossouw, D. Liles, R. Bittihn, and D. Hoge, J. Electrochem. Soc. 139, 363 (1992).
8. Y. Bando, S. Horii, and T. Takada, Jpn. J. Appl. Phys. 17, 1037 (1978).
9. K. A. Striebel, C. Z. Deng, S. J. Wen, and E. J. Cairns, J. Electrochem. Soc. 143, 1821 (1996).
10. F. K. Shokoohi, J. M. Tarascon, B. J. Wilkens, D. Guyomard, and C. C. Chang, J. Electrochem. Soc. 139, 1845 (1992).
11. A. Rougier, K. A. Striebel, S. J. Wen, and E. J. Cairns, J. Electrochem. Soc. 145, 2975 (1998).
12. N. J. Dudney, J. B. Bates, R. A. Zuhr, S. Young, J. D. Robertson, H. P. Jun, and S. A. Hackney, J. Electrochem. Soc. 146, 2455 (1999).
13. K. -H. Hwang, S. -H. Lee, and S. -K. Joo, J. Electrochem. Soc. 141, 3296 (1994).
14. P. Liu, J. G. Zhang, J. A. Turner, C. E. Tracy, and D. K. Benson, J. Electrochem. Soc. 146, 2001 (1999).
15. M. Isai, K. Yamaguchi, H. Iyoda, H. Fujiyasu, and Y. Ito, J. Mater. Res. 14, 1653 (1999).
16. M. Isai, K. Yamaguchi, T. Nakamura, Y. Ito, and H. Fujiyasu, Trans. Mater. Res. Soc. Jpn. 24, 157 (1999).
17. M. Isai, K. Yamaguchi, T. Nakamura, H. Fujiyasu, and Y. Ito, Proc. of the Sym. on Giga Scale Integration Technology, Washington State University, Pullman, Washington, Sep.28-29, pp.165-170 (1998). [Part of the 35th Annual Society of Engineering Science Meeting]
18. M. Isai, H. Ichikawa, T. Shimada, H. Fujiyasu, and Y. Ito, Trans. Mater. Res. Soc. Jpn. 25,1127(2000).
19. M. Isai, H. Ichikawa, T. Shimada, K. Morimoto, H. Fujiyasu, and Y. Ito, Jpn. J. Appl. Phys. 39, 6676 (2000).
20. M. Isai, H. Ichikawa, H. Takahashi, H. Fujiyasu, and Y. Ito, Electrochemistry, 68, 963 (2000).
21. M. Isai, T. Shimada, T. Matsui, H. Fujiyasu, Jpn. J. Appl. Phys. 40, 5069 (2001).
22. M. Isai and H. Fujiyasu, Jpn . J. Appl. Phys. 40, 6552 (2001).
23. for example: ASTM card No.24-734 or NBS Mono. 25, Sec. 10, 38 (1972).
24. J. F. Moulder, W. F. Strickle, P. E. Sobol and K. D. Bomben, Handbook of X-Ray Photoelectron Spectroscopy (Physical Electronics, Inc., Minnesota, 1995) p.79
25. M. Kumagai, S. Tanifuji and K. Tano, J. of Power Sources 35, 313 (1991).